Absolute Cross Sections for the Reactions $B^{11}(\gamma,2p)Li^9$ and $C^{12}(\gamma,3p)Li^9$†

G. W. TAUTFEST
Department of Physics, Purdue University, Lafayette, Indiana
(Received January 15, 1958)

Activation curves for the reactions $B^{11}(\gamma,2p)Li^9$ and $C^{12}(\gamma,3p)Li^9$ were obtained in the energy range 100–320 Mev. Targets of boron and carbon were exposed to the bremsstrahlung beam of the synchrotron and the yields of Li^9 measured by counting the delayed neturons in a moderator-counter assembly surrounding the targets. The activation curves were analyzed by the photon difference method to obtain the cross-section curves as a function of energy. Both cross sections show a pronounced increase above 150 Mev, and have integrated values up to 320 Mev of 2.0±0.3 Mev-millibarns for the reaction $B^{11}(\gamma,2p)Li^9$ and 0.31±0.05 Mev-millibarn for the reaction $C^{12}(\gamma,3p)Li^9$.

I. INTRODUCTION

EXPERIMENTS on photonuclear reactions involving the emission of more than one nucleon are comparatively rare because of the relative inaccessibility of the reactions to workers in the betatron energy range. Exceptions to this are the work of Halpern *et al.*[1] who, working with a 320-Mev bremsstrahlung beam, identified the products of multiple-nucleon emission from elements in the copper-arsenic group by chemical separations, and Reagan[2] who evaluated the yields of N^{17} from several elements as a function of energy in the range 80–400 Mev. The measurements of Halpern *et al.* established that even at 320 Mev, the the low-energy giant resonance contributed most of the yield for the emission of one or two nucleons. On the other hand, they found the pattern of the yields of more than two nucleons to be similar to that of high-energy particle-induced reactions. Reagan has found that the detailed activation curves of single and two-proton emission from O^{18} and F^{19}, respectively, confirm the previous results even for such light elements. For the emission of more than two nucleons, his activation curves indicate an ever-increasing cross section in the high-energy region.

In the work to be described we have used the technique developed by Reagan to confirm his conclusions regarding the excitation of the reactions $O^{18}(\gamma,p)N^{17}$ and $F^{19}(\gamma,2p)N^{17}$. We have found, however, that the excitation of the reaction $B^{11}(\gamma,2p)Li^9$ is qualitatively quite different from that of $F^{19}(\gamma,2p)N^{17}$ and suggest an explanation based on the higher threshold of the former reaction. The reaction $C^{12}(\gamma,3p)Li^9$ has also been reported by Reagan[3] and our activation curve is consistent with his single measurement at 270 Mev. However, we do not agree with his conclusion regarding the excitation of the reaction and obtain a much larger integrated cross section.

We have measured the yields of Li^9 resulting from photon bombardment of boron and carbon targets with bremsstrahlung of peak energy in the range 100–320 Mev. The activation curves have been analyzed and the photon cross sections obtained are compared with similar results obtained by others.

II. APPARATUS AND PROCEDURE

The Li^9 produced in the bombardments was detected by counting the delayed neutrons resulting from the beta decay of Li^9 to Be^{9*}. The reaction has been reported to have a half-life of 0.168 second[4] and to have a Q-value of 4.4 Mev.[5] The targets consisted of boron and carbon of natural isotopic abundance. The thickness of the boron target was measured to be 4.31 g/cm²; that of carbon, 26.6 g/cm². The targets were partially enclosed by a paraffin-moderated array of BF_3 proportional counters. The efficiency of the detecting system was evaluated with the working-standard Ra-Be source of the Argonne National Laboratory.[6] The absolute efficiency was measured to be 1.61% with an uncertainty in the measurement of 3%.

The source of photons used in the experiment was the Purdue University synchrotron with an internal target of 0.040-inch Pt wire. The energy of the synchrotron is determined by integration of the voltage induced in a coil of known area located in the magnet gap. This information together with the known radius at which the target is located affords a determination of energy; the uncertainty of this measurement is 3%. The energy of the electron beam is varied by turning off the rf acceleration and allowing the increasing magnetic field to shrink the orbit until the target is struck. Beam monitoring is done by a "Cornell-type" thick-walled ionization chamber. The charge collected by the chamber is integrated and measured by an automatic electronic slide-back electrometer.[7] The absolute monitor response has been determined by a Blocker-Kenney-Panofsky experiment[8] at peak brems-

† The research reported in this document was supported in part by the U. S. Atomic Energy Commission.
[1] Halpern, Debs, Eisinger, Fairhall, and Richter, Phys. Rev. **97**, 1327 (1955).
[2] Daryl Reagan, Phys. Rev. **100**, 113 (1955).
[3] Daryl Reagan, Phys. Rev. **92**, 651 (1953).
[4] Gardner, Knable, and Moyer, Phys. Rev. **83**, 1054 (1951).
[5] W. F. Fry, Phys. Rev. **89**, 325 (1953).
[6] We are indebted to Dr. E. W. Phelan of the Argonne National Laboratory for his assistance in arranging for the loan of this source and some of the BF_3 counters used in this experiment.
[7] R. Littauer, Rev. Sci. Instr. **25**, 148 (1954).
[8] Blocker, Kenney, and Panofsky, Phys. Rev. **79**, 419 (1950).

strahlung energies of 126, 191, 250, and 318 Mev. The experimental uncertainty of this measurement, based upon internal consistency only, is 5%.

The experimental arrangement is shown in Fig. 1. The photon beam exits from the synchrotron doughnut through a 0.005-inch Mylar window and is collimated by a 1.5-inch hole in a stack of $\frac{1}{16}$-inch lead sheets, 12 inches thick. Pictures of the beam taken at the target position show that at 100 Mev the beam almost fills the aperture, while at 320 Mev the intense central portion of the beam is approximately $\frac{1}{2}$ inch in diameter. The beam passes through the 3-inch hole in the moderator-counter assembly where the targets are placed and then strikes the ionization chamber.

The parallel outputs of the BF_3 counters are amplified and sent to the counting room. Here the pulses are put through an amplifier-discriminator and fed to the inputs of nine gated amplifiers. A series of phantastron gate generators applies gating pulses of variable delay and width to the amplifiers. The output of each amplifier is scaled. A diagram of the electronics arrangement is shown in Fig. 2. The sequence of operations is

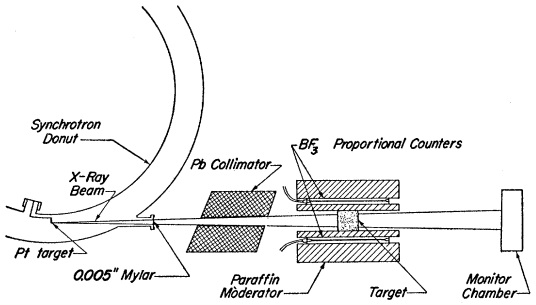

FIG. 1. Schematic diagram of the experimental setup.

as follows: the synchrotron is pulsed every 500 milliseconds, the magnet cycle being initiated by a pulse generated at zero time. Two to nine milliseconds later (depending on the energy desired) the electron beam strikes the target. Thirty milliseconds after the initiating pulse (to allow the prompt neutrons to disappear) the first amplifier is gated on for a period of 50 milliseconds; the second amplifier is then gated on for an identical period of time, and so on for all nine channels. This sequence is repeated until several thousand counts have been recorded in the first channel. The delayed neutrons are thus followed for a period of 2.68 half-lives to allow a measurement of the contamination of the yield. In the early stages of the experiment the decay was followed for 5.36 half-lives between beam pulses but the clean decay plots suggested that this was unnecessary. A plot of the neutron activity from the boron target at a peak bremsstrahlung energy of 320 Mev is given in Fig. 3. The background is evaluated by replacing the target with a copper absorber of identical thickness in radiation lengths. The background yields showed no variation from channel to

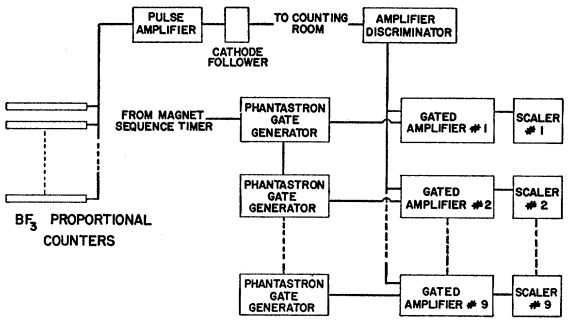

FIG. 2. Block diagram of electronics.

channel except for the first channel in which it was approximately 50% larger. For the carbon target at a peak bremsstrahlung energy of 100 Mev, the background was about equal to the signal; it was therefore, unprofitable to attempt to run at lower beam energy.

III. EXPERIMENTAL RESULTS

A. Activation Curves

The yield as a function of the peak bremsstrahlung energy k_0 is given by

$$Y(k_0)=N_tQ\int_{k_t}^{k_0}\sigma(k)\phi(k,k_0)dk, \qquad (1)$$

where $Y(k_0)$ is the number of Li^9 atoms produced for Q effective quanta incident on the target; N_t is the number of target nuclei per cm^2; $\sigma(k)$ is the reaction cross section at a photon energy k having a threshold at photon energy k_t; $\phi(k,k_0)$ is the photon distribution function. This yield is obtained from the number of delayed neutrons counted in all nine channels corrected for (1) the efficiency of the detector and (2) the counting

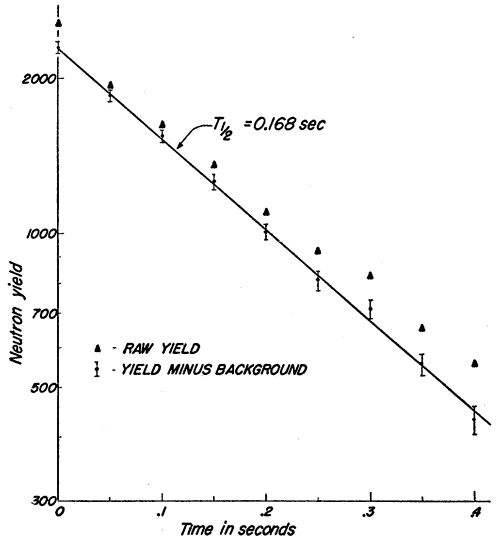

FIG. 3. Decay plot of neutrons from boron target bombarded with 320-Mev bremsstrahlung.

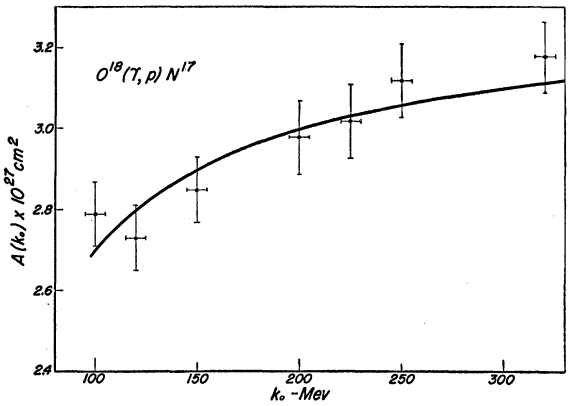

FIG. 4. Yield curve for the reaction $O^{18}(\gamma,p)N^{17}$. The solid curve is a 25-Mev isochromat corresponding to an integrated cross section of 58 Mev-millibarns.

duty-cycle. The number of effective quanta Q is obtained from the ionization-chamber calibration. For the water and carbon targets it was necessary to correct the ionization-chamber response for target absorption and scatter. This correction was measured by observing the ratio of the yield of a thin-walled ionization chamber placed ahead of the target position to the yield of the thick-walled ionization chamber for target-in and target-out. This correction was negligible for the boron and lithium-fluoride targets.

In order to check the functioning of the entire apparatus the excitations of the reactions $O^{18}(\gamma,p)N^{17}$ and $F^{19}(\gamma,2p)N^{17}$ were measured. An ordinary water target of thickness 17.8 g/cm^2 was used for the O^{18} and a LiF target, 9.10 g/cm^2 thick, for the F^{19}.

The activation cross sections obtained are shown in Figs. 4–7, where activation cross section is defined as

$$A(k_0)=\int_{k_t}^{k_0}\sigma(k)\phi(k,k_0)dk. \qquad (2)$$

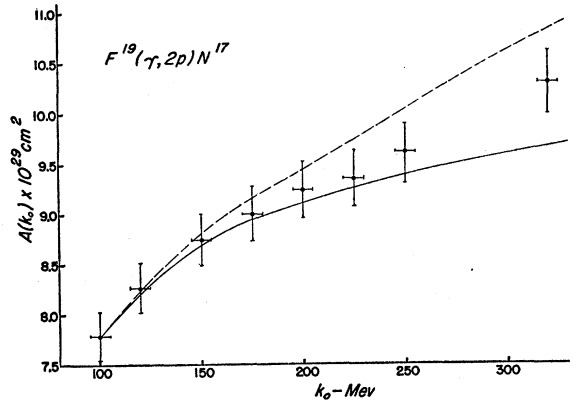

FIG. 5. Yield curve for the reaction $F^{19}(\gamma,2p)N^{17}$. The solid curve is a 40 Mev isochromat corresponding to an integrated cross section of 3.1 Mev-millibarns. The dashed curve shows the effect of adding a meson rise calculated from the cross section above 100 Mev in Fig. 8.

The errors indicated in the ordinates of the activation points are due to (1) the counting statistics (1–2%) (2) uncertainty in the monitor response as a function of energy (2–4%) (3) uncertainty in the absolute detection efficiency (3%). They do not include a possible systematic error in the absolute monitor response. The indicated errors in the abscissas are due to (1) uncertainty in the absolute energy calibration (3%) and (2) estimated uncertainty in the rf turn-off time (1–3%). All errors are standard deviations.

B. Cross-Section Curves

The cross sections were obtained from the activation curves by applying the photon difference method.[9] The spectral distribution was calculated from the Bethe-Heitler bremsstrahlung theory[10] modified by the method of Wilson[11] for the finite thickness of the radiator. We have made no direct measurement of the photon spectrum at this laboratory. Measurements of

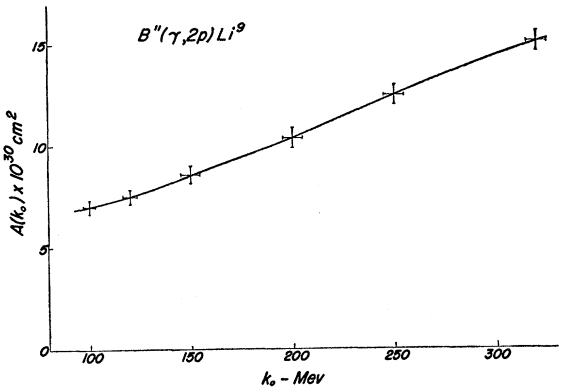

FIG. 6. Yield curve for the reaction $B^{11}(\gamma,2p)Li^9$. The solid curve is the yield curve constructed from the cross-section curve in Fig. 8.

the spectral distribution of synchrotron radiation[12–14] at other laboratories have shown no deviations from calculated distributions within the experimental errors.

Since no yield points were taken below 100 Mev, it was necessary to fit the yields at 100 Mev with arbitrary cross sections in this region. This arbitrariness adds the largest single uncertainty to the cross-section curves in spite of the small fraction of the cross sections existing below 100 Mev. The photon cross sections displayed do not directly reflect the errors in the activation points. Many such cross sections can be obtained which, although they differ in detail from each other, are more or less consistent with the data. The curves shown in

[9] L. Katz and A. G. W. Cameron, Can. J. Phys. **29**, 518 (1951).
[10] H. A. Bethe and W. Heitler, Proc. Roy. Soc. (London) **A146**, 83 (1934).
[11] R. Wilson, Proc. Roy. Soc. (London) **A66**, 638 (1953).
[12] Powell, Hartsough, and Hill, Phys. Rev. **81**, 213 (1951).
[13] J. W. DeWire and L. A. Beach, Phys. Rev. **83**, 476 (1951).
[14] D. H. Cooper, thesis, California Institute of Technology (unpublished).

Figs. 8 and 9 as a function of photon energy maximize the requirements of fit to the data and relatively smooth energy dependence.

IV. DISCUSSION OF RESULTS

The activation yields of the reactions $O^{18}(\gamma,p)N^{17}$ and $F^{19}(\gamma,2p)N^{17}$ as shown in Figs. 4 and 5 are fitted with yield curves based upon narrow resonances in the cross sections at 25 and 40 Mev, respectively, as suggested by Reagan.[2] The integrated values of the cross sections are 58±6 Mev-millibarns for oxygen and 3.1±0.4 Mev-millibarns for fluorine. These results are approximately 15% smaller than the measurements of Reagan, indicating a possible error in the absolute beam calibration of this experiment. A second possibility is that Reagan underestimated the amount of direct electron production which was present in his experiment.

A comparison of the activation curves for the $(\gamma,2p)$ reactions in B^{11} and F^{19} is of interest because they

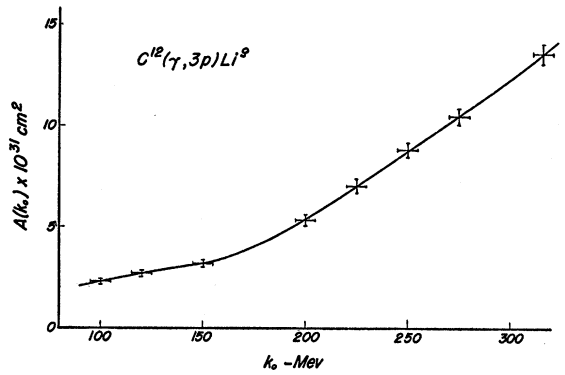

FIG. 7. Yield curve for the reaction $C^{12}(\gamma,3p)Li^9$. The solid curve is the yield curve constructed from the cross-section curve shown in Fig. 9.

might be expected to show similar behavior. If the dominance of the low-energy giant resonance which persists in F^{19} up to 320 Mev is the usual situation, as is suggested by the results of Halpern *et al.*,[1] then this mode of de-excitation must be abnormally small in the B^{11} nucleus below 100 Mev. Gell-Mann *et al.*[15] have derived a sum-rule result for the integrated gamma-absorption cross section up to meson threshold. Their result is

$$\int_0^{\mu}\sigma_T(k)dk=\frac{2\pi^2e^2\hbar}{Mc}\frac{NZ}{A}\left(1+0.1\frac{A^2}{NZ}\right)\text{ Mev-barns},\quad(3)$$

where μ is the pion rest energy and $\sigma_T(k)$ is the total gamma-absorption cross section. The ratio of the experimental yields of $B^{11}(\gamma,2p)$ and $F^{19}(\gamma,2p)$ at 150 Mev, normalized to the total integrated absorption cross sections evaluated from Eq. (3), is 1:10. A

[15] Gell-Mann, Goldberger, and Thirring, Phys. Rev. **95**, 1612 (1954).

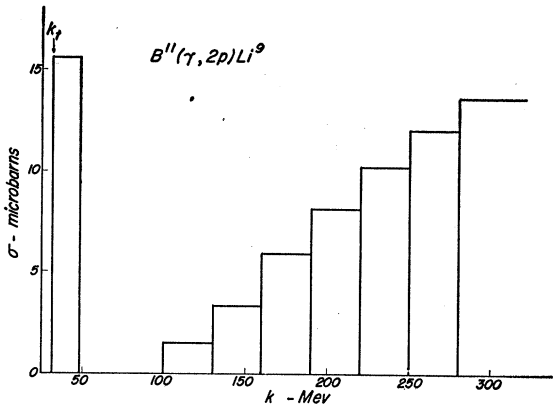

FIG. 8. Photon cross section for the reaction $B^{11}(\gamma,2p)Li^9$ obtained by the photon difference method from the yield points of Fig. 6. The photon cross section below 100 Mev was chosen arbitrarily.

consideration of the difference in threshold energies between the two nuclei is sufficient to explain this low value of the normalized ratio of yields.

The threshold for the $(\gamma,2p)$ reaction in F^{19} is 23.5 Mev; in B^{11}, 31.3 Mev. The (γ,n) thresholds are almost the same. This suggests, therefore, that at a photon energy at which the $(\gamma,2p)$ reaction is able to compete in B^{11}, there is little or no absorption cross section left. The threshold is far down in the tail of the absorption resonance, in contrast to the situation in F^{19}. It is only at photon energies for which the absorption cross section once more increases because of meson interactions that the $(\gamma,2p)$ yield in B^{11} attains a value relative to the total integrated absorption cross section comparable to that existing in the giant resonance region in F^{19} (the ratio of the normalized yields is 1:1 at 320 Mev).

The photon cross section obtained for the $B^{11}(\gamma,2p)Li^9$ reaction above 100 Mev (see Fig. 8) was multiplied by the ratio of the total integrated absorption cross sections calculated from Eq. (3) for F^{19} and B^{11} and used to calculate an activation yield for the $F^{19}(\gamma,2p)N^{17}$ reaction which is in addition to the yield from the giant

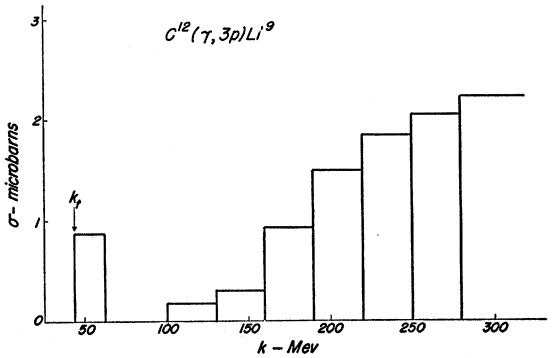

FIG. 9. Photon cross section for the reaction $C^{12}(\gamma,3p)Li^9$ obtained by the photon difference method from the yield points of Fig. 7. The photon cross section below 100 Mev was chosen arbitrarily.

resonance. The result is the dashed curve shown in Fig. 5. It can be seen that the experimental yield points suggest that this perhaps overestimates the meson rise in the yield by about a factor of two. In any case, the integrated cross section for the $F^{19}(\gamma,2p)N^{17}$ reaction up to 320 Mev should probably be increased to at least 3.3 ± 0.4 Mev-millibarns. The integral of the $B^{11}(\gamma,2p)Li^{9}$ cross section up to 320 Mev has the value 2.0 ± 0.3 Mev-millibarns. These errors are the rms deviations in the cross sections allowed by the errors in the activation yield points.

The $(\gamma,3p)$ cross section in C^{12} shown in Fig. 9 is in qualitative agreement with the measurements of similar reactions obtained by Halpern *et al.*[1] and Reagan.[2] The cross-section curve indicates that most of the cross section lies above 100 Mev. This is contrary to the assertion of Reagan[3] that the reaction excites like $F^{19}(\gamma,2p)N^{17}$. The source of this discrepancy is not clear. The cross section integrated to 320 Mev has the value 0.31 ± 0.05 Mev-millibarn.

ACKNOWLEDGMENTS

The author wishes to acknowledge many helpful discussions with Professor T. R. Palfrey and Professor D. C. Peaslee. He is indebted to the synchrotron operators, E. Metcalf and L. Gordon, for the efficient operation of the accelerator and to R. Carter and H. Wilson for assistance in data collection.

PHYSICAL REVIEW VOLUME 110, NUMBER 3 MAY 1, 1958

Atomic Masses from Phosphorus through Manganese*

CLAYTON F. GIESE† AND JAY L. BENSON
School of Physics, University of Minnesota, Minneapolis, Minnesota
(Received January 6, 1958)

Atomic masses of all the stable isotopes of the elements from phosphorus through manganese have been measured with the large double-focusing mass spectrometer at this laboratory.

The comparison with previous mass spectroscopic results presents a varying pattern of agreement and disagreement. The agreement of the present mass measurements with results from microwave spectroscopy is, in general, good. The present masses agree much better with Q-value determinations than do previous masses. The remaining differences appear to be systematic. It would appear to be symptomatic of the discrepancies that in all cases, 10 in number, in which a (p,α) Q-value can be predicted from the present measured masses, the measured Q-value is less than the predicted value.

The present paper includes a tabulation of masses of unstable nuclei. In addition, tables and plots of nucleon separation and total nucleon pairing energies for this mass region are included.

INTRODUCTION

RECENT measurements of atomic masses at this laboratory using a double-focusing mass spectrometer have covered the regions from boron through silicon[1,2] and from iron through zinc.[3] The present work fills in the gap between these previous sets of measurements.

Most of the masses in this region have been determined before, both mass-spectroscopically and by calculations based on Q-values. Certain mass ratios have been determined by microwave spectroscopy. However, the agreement between mass-spectroscopic masses and Q-value masses has not been good in a number of cases. In addition, it would seem that a large block of connected mass data would be of the greatest value in any study of the systematics of nuclear masses as well as in a search for systematic errors in the mass-spectroscopic or Q-value masses. For these reasons it has seemed desirable to undertake the measurements reported in the present paper.

The masses measured include S^{36}, which had been determined previously only by microwave spectroscopy, and Ca^{46}, which had never been measured.

MEASUREMENTS

The mass spectrometer and the method of measurement of the mass doublets have been described in some detail in other reports.[1] The enriched KCl used in the potassium measurements was obtained from the Oak Ridge National Laboratory and had the following isotopic abundances: K^{39}, 63.1%; K^{40}, 7.8%; K^{41}, 29.2%. Enriched argon available at this laboratory was used for the measurements of A^{36} and A^{38}. All other measurements were made using samples having the natural abundances of isotopes.

The Ti^+, V^+, and Cr^+ ions were obtained, respectively, from the vapor of $TiCl_4$, $VOCl_3$, and CrO_2Cl_2. Because of the rather high reactivity of these liquids, a greaseless leak system was required. The adjustable leak used was simply a commercial Monel vacuum

* Research supported by the joint program of the U. S. Atomic Energy Commission and the Office of Naval Research.
† National Science Foundation Predoctoral Fellow 1954–1957. Now at the University of Chicago, Chicago, Illinois.
[1] Quisenberry, Scolman, and Nier, Phys. Rev. **102**, 1071 (1956).
[2] Scolman, Quisenberry, and Nier, Phys. Rev. **102**, 1076 (1956).
[3] Quisenberry, Scolman, and Nier, Phys. Rev. **104**, 461 (1956).